AIAA JOURNAL
Vol. 38, No. 9, September 2000

Nonlinear Response of Composite Panels Under Combined Acoustic Excitation and Aerodynamic Pressure

K. Abdel-Motagaly,* B. Duan,* and C. Mei†
Old Dominion University, Norfolk, Virginia 23529-0247

A finite element formulation is presented for the analysis of the large deflection response of composite panels subjected to high acoustic excitation and aerodynamic pressure at supersonic flow. The first-order shear deformation theory is considered for laminated composite plates, and the von Kármán nonlinear strain–displacement relations are employed for panel large deflection response. The first-order piston theory aerodynamics and the simulated Gaussian white noise are employed for the aerodynamic and acoustic loads, respectively. The nonlinear equations of motion for an arbitrarily laminated composite panel subjected to combined aerodynamic and acoustic pressures are formulated first in structure node degrees of freedom. The system equations are then transformed and reduced to a set of coupled nonlinear equations in modal coordinates. Modal participation is defined and the in vacuo modes to be retained in the analysis are based on the modal participation values. Numerical results include root mean square values of maximum deflections, deflection and strain response time histories, probability distributions, power spectrum densities, and skewness and kurtosis. Results showed that combined acoustic and aerodynamic loads have to be considered for panel analysis and design at high dynamic pressure values.

I. Introduction

AIRCRAFT and spacecraft skin panels are subjected simultaneously to high levels of acoustic (sonic fatigue) and aerodynamic (panel flutter) pressures.[1,2] Sonic fatigue and panel flutter have been the major design consideration for aircraft, spacecraft, and missiles since the late 1960s. An excellent review of sonic fatigue technology up to 1989 was given by Clarkson.[3] Various types of pressure loads, developments of theoretical methods, comparisons of experimental results with theories, and monographs were given. Recently, Wolfe et al.[4] gave reviews of sonic fatigue design guides, classical and finite element approaches, and identification technology. Experimental investigation of nonlinear beams and plates and a multimodal fatigue model were also reported. Sonic fatigue design guides have been developed by Rudder and Plumblee[5] for isotropic metallic and by Holehouse[6] for graphite–epoxy composite aircraft structures. The design guides, however, were based on the semiempirical test data or the simplified single-mode approach. Vaicaitis has developed a Galerkin-like procedure [partial differential equation (PDE) and modal method] and a time-domain Monte Carlo approach for the nonlinear response of isotropic[1,2] and composite panels (Arnold and Vaicaitis[7] and Vaicaitis and Kavallieratos[8]) to acoustic and thermal loads. However, combined acoustic and aerodynamic loads were not investigated.

An excellent survey of nonlinear panel flutter through 1970 was given by Dowell.[9] The vast amount of theoretical literature on panel flutter was grouped into four categories based on the linear or nonlinear structure theories and the two aerodynamic theories (quasi-steady first-order piston or full linearized inviscid potential flow). The numerical results from the PDE and the Galerkin's method showed that a minimum of six modes are needed for a converged limit cycle amplitude response for a simply supported square isotropic panel. Bismarck-Nasr gave reviews of the linear[10] and nonlinear[11] panel flutter using the finite element methods. Recently, a review of various analytical methods of nonlinear panel flutter at supersonic and hypersonic speeds was given by Mei et al.[12] An approach for the design of flutter-free surface panels using the quasi-static Ackeret aerodynamic theory was documented by Laurenson and McPherson.[13] An exhaustive search reveals that there is no study of nonlinear panel response to combined acoustic and aerodynamic loads in the literature.

When a vehicle travels at supersonic speeds, flutter caused by aerodynamic pressure is not the only form of dynamic instability. The surface panels also experience high-frequency random pressure fluctuations (sonic fatigue). This paper presents a finite element formulation for the analysis of nonlinear large deflection response of composite panels subjected to high acoustic excitation and aerodynamic pressure. The first-order shear deformation theory is considered for the laminated composite plates. The von Kármán nonlinear strain–displacement relations are employed for the large deflection response of the panel. Simulated Gaussian white noise and the first-order piston theory aerodynamics are employed for the acoustic and aerodynamic loads. The nonlinear equations of motion for an arbitrarily laminated composite panel subjected to combined high acoustic and aerodynamic loads are formulated first in the structure node degrees of freedom (DOF). The system equations are then transformed and reduced to a set of coupled nonlinear equations in modal coordinates. Numerical integration is employed to obtain the panel response. Examples are given for an isotropic and a composite panel at various combinations of sound pressure level and dynamic pressure.

II. Formulation

A. Equations of Motion in Structure Node DOF

The inplane strain, curvature, and shear strain vectors based on the von Kármán large deflection and the first-order shear deformation theories are given by

$$\{\varepsilon^0\} = \{\varepsilon_m^0\} + \{\varepsilon_b^0\} = \begin{Bmatrix} u_{,x} \\ v_{,y} \\ u_{,y} + v_{,x} \end{Bmatrix} + \begin{Bmatrix} w_{,x}^2/2 \\ w_{,y}^2/2 \\ w_{,x}w_{,y} \end{Bmatrix}$$

$$\{\kappa\} = \begin{Bmatrix} \psi_{x,x} \\ \psi_{y,y} \\ \psi_{x,y} + \psi_{y,x} \end{Bmatrix}, \qquad \{\gamma\} = \begin{Bmatrix} w_{,y} + \psi_y \\ w_{,x} + \psi_x \end{Bmatrix} \tag{1}$$

where u, v, and w are the inplane and transverse displacements, respectively, and Ψ_x and Ψ_y are the rotations of the normal to the midsurface about the y and x axes, respectively. The subscripts m and b denote membrane (in-plane) and bending components, respectively. The constitutive equations for a laminated composite plate are

Presented as Paper 99-1380 at the AIAA/ASME/ASCE/AHS/ASC 40th Structures, Structural Dynamics, and Materials Conference, St. Louis, MO, 12–15 April 1999; received 4 June 1999; revision received 12 January 2000; accepted for publication 16 February 2000.

*Graduate Research Assistant, Department of Aerospace Engineering. Student Member AIAA.

†Professor, Department of Aerospace Engineering. Associate Fellow AIAA.

$$\begin{Bmatrix} N \\ M \end{Bmatrix} = \begin{bmatrix} A & B \\ B & D \end{bmatrix} \begin{Bmatrix} \varepsilon^0 \\ \kappa \end{Bmatrix}, \qquad \{Q\} = [A_s]\{\gamma\} \tag{2}$$

where $[A]$, $[B]$, $[D]$, and $[A_s]$ are the stretching, bending–stretching coupling, bending, and shear stiffnesses, respectively. The quasi-steady first-order piston aerodynamic theory is employed for the aerodynamic pressure at high supersonic Mach number ($M_\infty > 1.6$). The aerodynamic pressure is given by[9]

$$\Delta p = -\frac{2q_a}{\beta}\left(w_{,x} + \frac{M_\infty^2 - 2}{M_\infty^2 - 1}\frac{1}{V_\infty}w_{,t}\right) \tag{3}$$

where $q_a = \rho_a V_\infty^2/2$ is the freestream dynamic pressure, ρ_a is the air density, V_∞ is the velocity, and $\beta = \sqrt{(M_\infty^2 - 1)}$.

When we use the Hamilton's principle and the finite element expressions, the system equations of motion for a composite plate subjected to aerodynamic pressure[14] and acoustic excitation[15] can be expressed as

$$\left(1/\omega_0^2\right)[M]_b\{\ddot{W}_b\} + (g_a/\omega_0)[G]\{\dot{W}_b\} + ([K_L] + [K_{NL}])\{W_b\} = \{P_b(t)\} \tag{4}$$

where $\omega_0 = (D_{110}/\rho h a^4)^{1/2}$ is a reference frequency and ρ, h, and a are the panel density, thickness, and length, respectively. The value D_{110} is the first entry in laminate bending rigidity $[D]$ calculated when all of the fibers of the composite layers are aligned in the airflow x direction. The $[M]_b$, $[G]$, and $\{P_b\}$ are the system mass matrix, aerodynamic damping matrix, and load vector due to random acoustic pressure, respectively. The linear and nonlinear system stiffness matrices are given by

$$[K_L] = \lambda[A_a] + [K]_b + [K_s] - [K_B][K]_m^{-1}[K_B]^T$$

$$[K_{NL}] = -[K_B][K]_m^{-1}[K1]_{mb} + [K1_B] + [K1_{\mathrm{Nm}}] + [K1_{Nb}] + [K2] - [K1]_{bm}[K]_m^{-1}\left([K_B]^T + [K1]_{mb}\right) \tag{5}$$

where the nondimensional dynamic pressure and nondimensional aerodynamic damping are given by

$$\lambda = \left(2q_a a^3/\beta D_{110}\right), \qquad g_a = \sqrt{\lambda C_a} \tag{6}$$

where $C_a = \mu(M_\infty^2 - 2)^2/\beta(M_\infty^2 - 1)^2$ is the aerodynamic coefficient and $\mu = \rho_a a/\rho h$ is the mass ratio. For high supersonic speeds $M_\infty \gg 1$, Dowell[9] approximated $C_a \approx \mu/M_\infty$. The $[A_a]$ is the system aerodynamic influence matrix, and $[K1]$ and $[K2]$ are the first- and second-order nonlinear stiffness matrices that depend linearly and quadratically on the unknown system displacement vector $\{W\} = \{\{W_b\}, \{W_m\}\}^T$. The subscripts B, N_m, and N_b denote that the corresponding stiffness matrix is due to the laminate bending–stretching stiffness $[B]$, membrane force components $\{N_m\} = [A]\{\varepsilon_m^0\}$ and $\{N_b\} = [B]\{\kappa\}$, respectively, and the subscripts a and s denote aerodynamic and shear deformation, respectively. The derivation of Eq. (4) can be found in Refs. 14 and 15. In the absence of acoustic loading, $\{P_b(t)\} = 0$, Eq. (4) reduces to nonlinear panel flutter at supersonic speeds; however, by setting $\lambda = g_a = 0$, Eq. (4) describes nonlinear random response of a composite panel subjected to high acoustic excitations. To the authors' knowledge, this is the first attempt at investigating the nonlinear response of panels subjected to combined acoustic and aerodynamic pressures.

For a given set of λ and C_a (or μ/M_∞), Eq. (4) can be solved by numerical integration in the structure node DOF. This approach has been carried out with simulated random loads for sonic fatigue analysis.[16,17] It turned out to be computationally costly because 1) at each time step, the element nonlinear stiffness matrices are evaluated and the system nonlinear stiffness matrix $[K_{NL}]$ is assembled and updated, 2) the number of structure node DOF of $\{W_b\}$ is usually very large, and 3) the time step of integration should be extremely small.

An efficient solution procedure is to transform Eq. (4) into the modal coordinates[14] with a modal reduction. This is presented as follows.

B. Equations of Motion in Modal Coordinates

Express the panel deflection as a linear combination of some known functions as

$$\{W_b\} = \sum_{r=1}^{n} q_r(t)\{\phi_r\} = [\Phi]\{q\} \tag{7}$$

where the number of retained linear in vacuo modes n is much smaller than the number of structure node DOF in bending $\{W_b\}$. The normal mode $\{\phi_r\}$, which is normalized with the maximum component to unity, and the linear natural frequency ω_r are obtained from the linear vibration of the system

$$\left(\omega_r^2/\omega_0^2\right)[M]_b\{\phi_r\} = \left([K]_b + [K_s] - [K_B][K]_m^{-1}[K_B]^T\right)\{\phi_r\} \tag{8}$$

A small number of the most contributing modes to be retained in the analysis can be determined from the modal participation value, which is defined as

$$\text{participation of the } r\text{th mode} = \frac{\mathrm{rms}(q_r)}{\sum_{s=1}^{n}\mathrm{rms}(q_s)} \tag{9}$$

Because matrices $[K1]_{mb}$, $[K1_B]$, $[K1_{Nb}]$, and $[K2]$ are all functions of the unknown bending DOF $\{W_b\}$, they can now be expressed as the sum of products of modal coordinates and nonlinear modal stiffness matrices as

$$([K1]_{mb}, [K1_B], [K1_{Nb}], [K2]) = \sum_{r=1}^{n} q_r\left([K1]_{mb}^{(r)}, [K1_B]^{(r)}, [K1_{Nb}]^{(r)}, \sum_{s=1}^{n} q_s[K2]^{(rs)}\right) \tag{10}$$

where the superindices of those nonlinear modal stiffness matrices denote that they are assembled from the corresponding element nonlinear stiffness matrices. Those element nonlinear stiffness matrices are evaluated with the corresponding element components $\{w_b\}^{(r)}$ obtained from the known system linear mode $\{\phi_r\}$. Therefore, the nonlinear modal stiffness matrices are constant matrices. The matrix $[K1_{\mathrm{Nm}}]$, however, is a linear function of the inplane DOF $\{W_m\}$ that consists of two terms as

$$\{W_m\} = -[K]_m^{-1}\left([K_B]^T + [K1]_{mb}\right)\{W_b\} = -[K]_m^{-1}\left([K_B]^T + \sum_{s=1}^{n} q_s[K1]_{mb}^{(s)}\right)\sum_{r=1}^{n} q_r\{\phi_r\} = -\sum_{r=1}^{n} q_r\{\phi_r\}_m - \sum_{r=1}^{n}\sum_{s=1}^{n} q_r q_s\{\phi_{rs}\}_m \tag{11}$$

where the two inplane modes corresponding to the rth bending mode $\{\phi_r\}$ are given by

$$\{\phi_r\}_m = [K]_m^{-1}[K_B]^T\{\phi_r\}, \qquad \{\phi_{rs}\}_m = [K]_m^{-1}[K1]_{mb}^{(s)}\{\phi_r\} \tag{12}$$

The nonlinear stiffness matrix $[K1_{\mathrm{Nm}}]$ can be expressed as the sum of two nonlinear modal stiffness matrices as

$$[K1_{\mathrm{Nm}}] = -\sum_{r=1}^{n} q_r[K1_{\mathrm{Nm}}]^{(r)} - \sum_{r=1}^{n}\sum_{s=1}^{n} q_r q_s[K2_{\mathrm{Nm}}]^{(rs)} \tag{13}$$

The nonlinear modal stiffness matrices $[K1_{\mathrm{Nm}}]^{(r)}$ and $[K2_{\mathrm{Nm}}]^{(rs)}$ are constant matrices, and they are assembled and evaluated with the known inplane modes $\{\phi_r\}_m$ and $\{\phi_{rs}\}_m$, respectively. Equation (4) is thus transformed to the reduced modal coordinates as

$$\left(1/\omega_0^2\right)[\bar{M}]_b\{\ddot{q}\} + (g_a/\omega_0)[\bar{G}]\{\dot{q}\} + 2\xi_r\omega_r\left(\bar{M}_r/\omega_0^2\right)[I]\{\dot{q}\} + (\overline{[K_L]} + [K_q] + [K_{qq}])\{q\} = \{\bar{P}(t)\} \tag{14}$$

where the modal matrices are given by

$$([\bar{M}]_b, [\bar{G}], \overline{[K_L]}) = [\Phi]^T([M]_b, [G], [K_L])[\Phi] \tag{15}$$

Table 1 Comparison of rms of (W_{max}/h) for a simply supported rectangular (15 × 12 × 0.040 in.) isotropic plate with different methods and mode numbers

SPL, dB	FPK[19] 1 mode	FE/EL[20] 1 mode	FE/EL[20] 4 modes	Present 4 modes
90	0.249	0.238	0.238	0.266
100	0.592	0.532	0.533	0.489
110	1.187	1.030	1.031	1.092
120	2.200	1.902	1.905	2.113

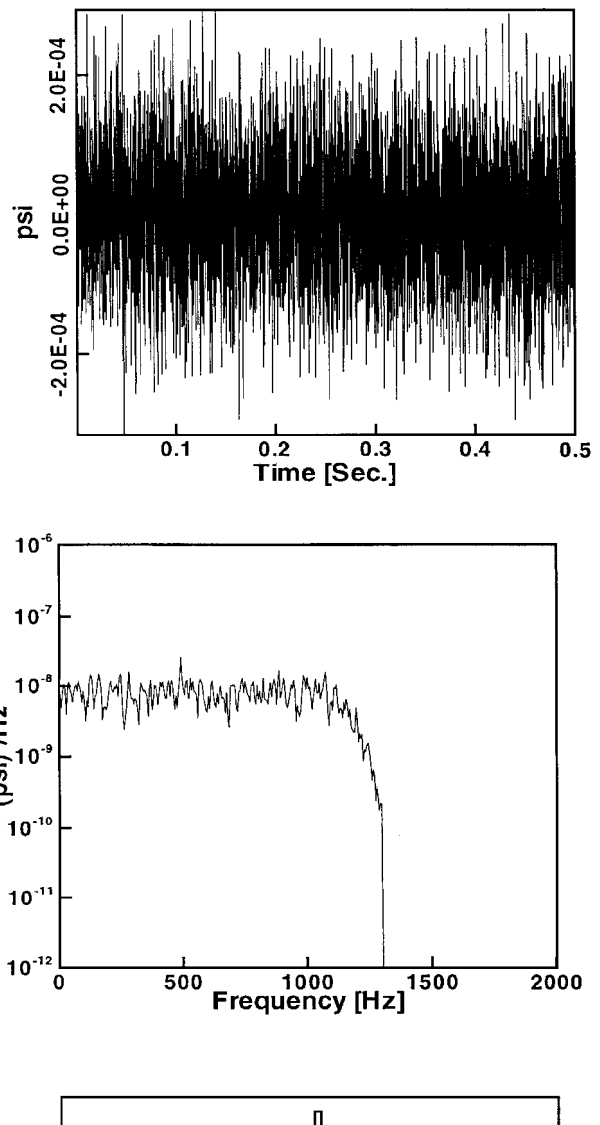

Fig. 1 Simulated input load.

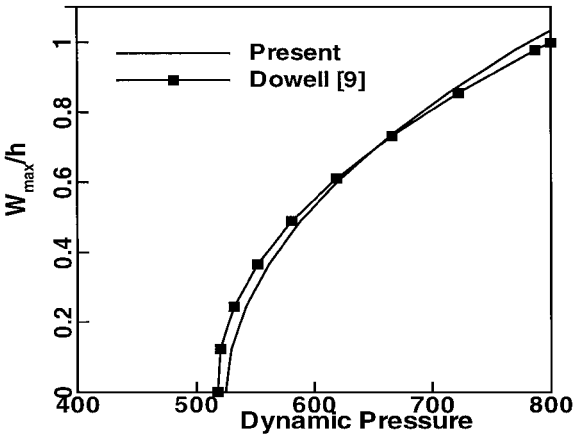

Fig. 2 Comparison of limit cycle amplitude for a simply supported square isotropic plate.

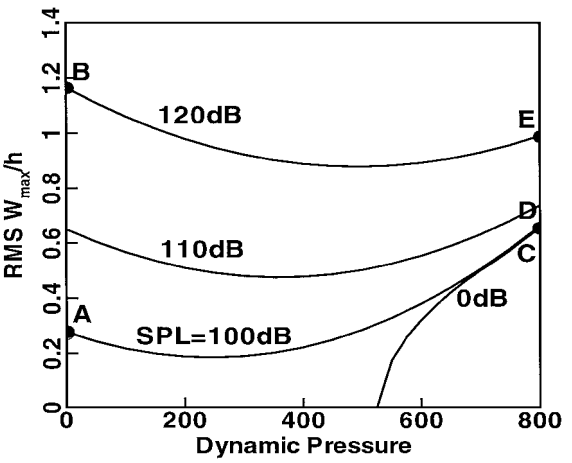

Fig. 3 Simply supported square isotropic plate rms maximum deflection.

and the quadratic and cubic terms are

$$[K_q]\{q\} = [\Phi]^T \sum_{r=1}^{n} q_r \Big(-[K_B][K]_m^{-1}[K1]_{mb}^{(r)} + [K1_B]^{(r)} - [K1_{\mathrm{Nm}}]^{(r)} + [K1_{Nb}]^{(r)} - [K1]_{bm}^{(r)}[K]_m^{-1}[K_B]^T\Big)[\Phi]\{q\}$$

$$[K_{qq}]\{q\} = [\Phi]^T \sum_{r=1}^{n}\sum_{s=1}^{n} q_r q_s \Big([K2]^{(rs)} - [K2_{\mathrm{Nm}}]^{(rs)} - [K1]_{bm}^{(r)}[K]_m^{-1}[K1]_{mb}^{(s)}\Big)[\Phi]\{q\} \tag{16}$$

and the modal force is

$$\{\bar{P}(t)\} = [\Phi]^T\{P_b(t)\} \tag{17}$$

A structural modal damping matrix $2\xi_r\omega_r(\bar{M}_r/\omega_0^2)[I]$ has been added to Eq. (14), and ξ_r is the modal damping ratio that can be determined experimentally or from the database of structures of similar construction. The nonlinear response for a given panel at certain dynamic pressure λ and damping parameters C_a and ξ_r can be determined from Eq. (14) by any numerical integration scheme. The advantages in using Eq. (14) are 1) there is no need to assemble the quadratic and cubic nonlinear terms because all the nonlinear modal matrices are constant matrices and 2) the number of modal equations n is small. This approach has been successfully carried out for nonlinear flutter of composite panels at an elevated temperature.[14]

C. Random Surface Pressure

The input acoustic excitation is assumed to be a band-limited Gaussian random noise and uniformly distributed over the structural

surface. The simulated time history, probability density, and power spectrum density (PSD) of the input are shown in Fig. 1. The PSD has the form

$$S(f) = p_0^2 10^{\mathrm{SPL}/10} \qquad 0 \le f \le f_c$$
$$= 0 \qquad \text{otherwise} \qquad (18)$$

where p_0 is the reference pressure, $p_0 = 2.9 \times 10^{-9}$ psi (20 μPa), sound pressure level (SPL) is the sound spectrum level in decibels, and f_c is the selected bandwidth. The formulation presented in Eq. (14), however, is not limited to stationary Gaussian excitation. It can also handle nonstationary, non-Gaussian random loads, which the high-speed flight vehicles would probably experience. With recorded flight high-frequency pressure fluctuations, random panel response can be determined much more realistically by numerical integration of Eq. (14).

III. Examples and Discussion

The nonlinear system equations presented in Eq. (4) are general in the sense that they are applicable for rectangular[14,16] or triangular[15] finite elements. The finite element employed in the examples is the three-node triangular Mindlin (MIN3) plate element with improved transverse shear.[18] The shear correction factor is defined as

$$\alpha_s = 1 \Big/ \left(1 + 0.5 \sum_{i=4,9} k_{sii} \Big/ \sum_{i=4,9} k_{bii} \right)$$

The MIN3 element has a total of 15 DOF, 5 at each apex node. The bending node DOF $\{w_b\}$ comprises transverse displacements and normal rotations w, Ψ_x, and Ψ_y and the in-plane node DOF $\{w_m\}$ comprises in-plane displacements u and v. Nonlinear responses are obtained for a square isotropic plate and a rectangular composite plate. An aerodynamic coefficient $C_a = 0.01$ and a modal damping ratio $\xi_r = 0.01$, $r = 1$ to n are used in the examples.

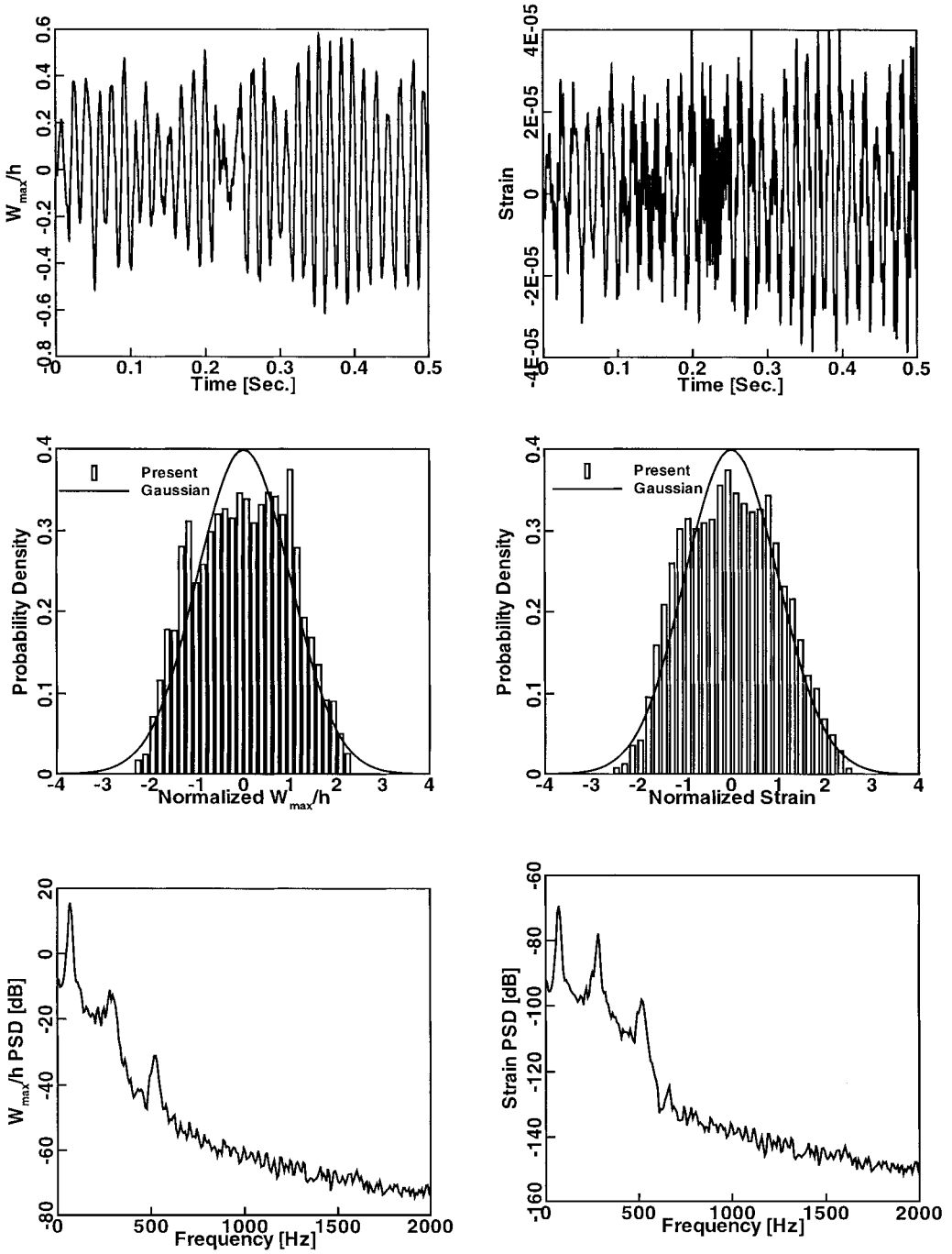

Fig. 4 Random response of a simply supported square isotropic plate at 100 dB SPL and $\lambda = 0$.

A. Validation

The accuracy of the present formulation is first verified and shown in Fig. 2 and Table 1 for panel flutter and sonic fatigue, respectively. For panel flutter, the plate is of $12 \times 12 \times 0.040$ in. ($30.5 \times 30.5 \times 0.1$ cm) with immovable inplane edges, $u(0, y) = u(a, y) = v(x, 0) = v(x, a) = 0$. The plate is modeled with a 12×12 mesh or 288 MIN3 elements. The number of structural node DOF $\{W_b\}$ is 407 for the system equations given in Eq. (4). It is well known that six modes in the airflow direction are needed for a converged limit cycle response and, thus, modes (1, 1)–(6, 1) are used in Eq. (14). For random response, the plate is of $15 \times 12 \times 0.040$ in. ($38.1 \times 30.5 \times 0.1$ cm) with immovable inplane edges. The material properties are $E = 10$ Msi (68.9 GPa) and $\nu = 0.3$. The lowest four symmetrical modes are included for the uniform input random pressure distribution analysis. The Fokker–Planck–Kolmogorov (FPK) equation[19] method is an exact solution to the single DOF forced Duffing equation. The finite element/equivalent linearization (FE/EL) approach[20] assumes that the equivalent linearized system obtained after the application of the equivalent linearization technique[21] is also stationary Gaussian, whereas the present time domain numerical integration method does not assume that the displacement response is Gaussian, therefore, the present method should be more accurate and realistic.

B. Square Isotropic Plate

The simply supported square plate for panel flutter in Fig. 2 is now studied in detail. The modes considered are (1, 1)–(6, 1) for panel flutter and (1, 1), (1, 3), (3, 1), and (3, 3) for sonic fatigue. No modal participation calculations are needed for this well-studied problem. The rms maximum deflections to plate thickness vs the nondimensional dynamic pressure λ at SPL of 0, 100, 110, and 120 dB are shown in Fig. 3. The curve with the null acoustic pressure (0-dB SPL) represents the conventional panel flutter limit cycle oscillations, and the rms deflections at null dynamic pressure ($\lambda = 0$) are the conventional nonlinear panel responses to acoustic excitations.

The maximum deflection is located at the three-quarter length from the leading edge ($3a/4$, $a/2$) for panel flutter; however, it is at the plate center ($a/2$, $a/2$) for sonic fatigue. For a fixed SPL, the

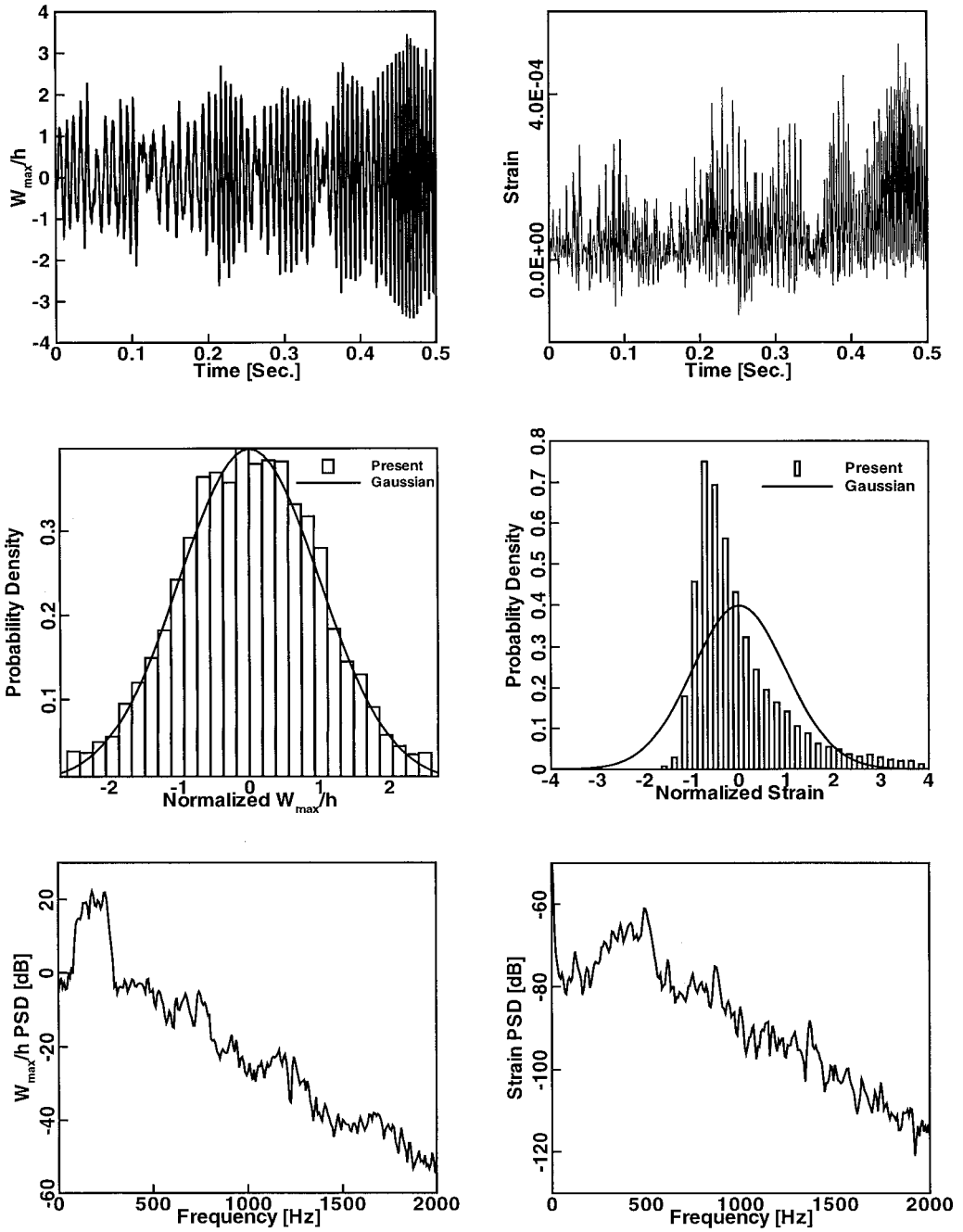

Fig. 5 Random response of a simply supported square isotropic plate at 120 dB SPL and $\lambda = 0$.

location of the maximum deflection thus moves from the plate center toward the three-quarter length as the dynamic pressure increases. However, for a fixed dynamic pressure, the location of the maximum deflection moves toward the center from the three-quarter length by increasing the SPL. The maximum deflection for the combined acoustic and aerodynamic loading case, therefore, is not at one fixed location, it could be somewhere between the plate center and three-quarter from the leading edge.

The deflection results shown in Fig. 3 indicate that 1) the superposition method is not applicable to nonlinear system, 2) a stiffening effect results from the aerodynamic load, so that the rms deflection initially decreases with increasing dynamic pressure λ, then begins increasing when λ approach λ_{cr}, and 3) the rms deflections at large dynamic pressure ($\lambda \gg \lambda_{cr}$) are always higher than those at $\lambda = 0$. Important conclusions can be drawn for design and analysis of surface panels at supersonic speeds: 1) for $\lambda \ll \lambda_{cr}$, only acoustic loading or sonic fatigue has to be considered, 2) for significant λ, but $\lambda < \lambda_{cr}$, both acoustic and aerodynamic loads must be considered, as consideration of acoustic loads alone would result in an overly conservative design, and 3) for $\lambda > \lambda_{cr}$, both acoustic and aerodynamic loads have to be considered because consideration of acoustic loads alone would lead to a nonconservative design.

Representative panel behaviors at five loading combinations are presented in Figs. 4–8. Those five loading combinations correspond to A–E shown in Fig. 3. The maximum deflection and maximum strain response time histories, probability distribution, and PSD for each loading case are presented. Tables 2 and 3 present the maximum deflection and maximum strain response statistical moments for the five loading cases. The skewness and kurtosis coefficients are defined as

$$\text{skewness} = \mu_3/\sigma^3, \qquad \text{kurtosis} = \left(\mu_4/\sigma^4\right) - 3 \tag{19}$$

where μ_k and σ denote the kth central moment and standard deviation, respectively. Figures 4 and 5 show the random response at

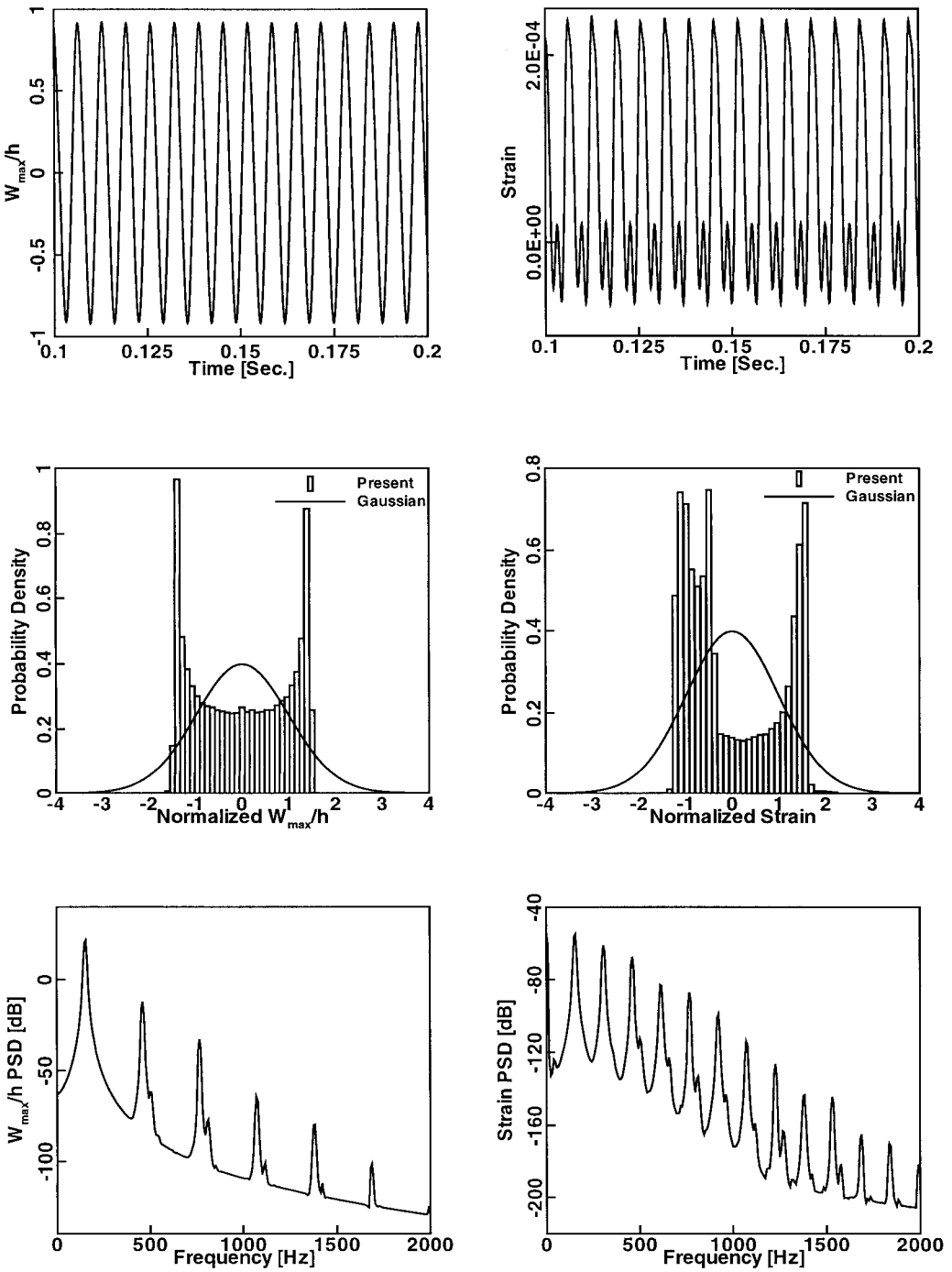

Fig. 6 Random response of a simply supported square isotropic plate at 0 dB SPL and $\lambda = 800$.

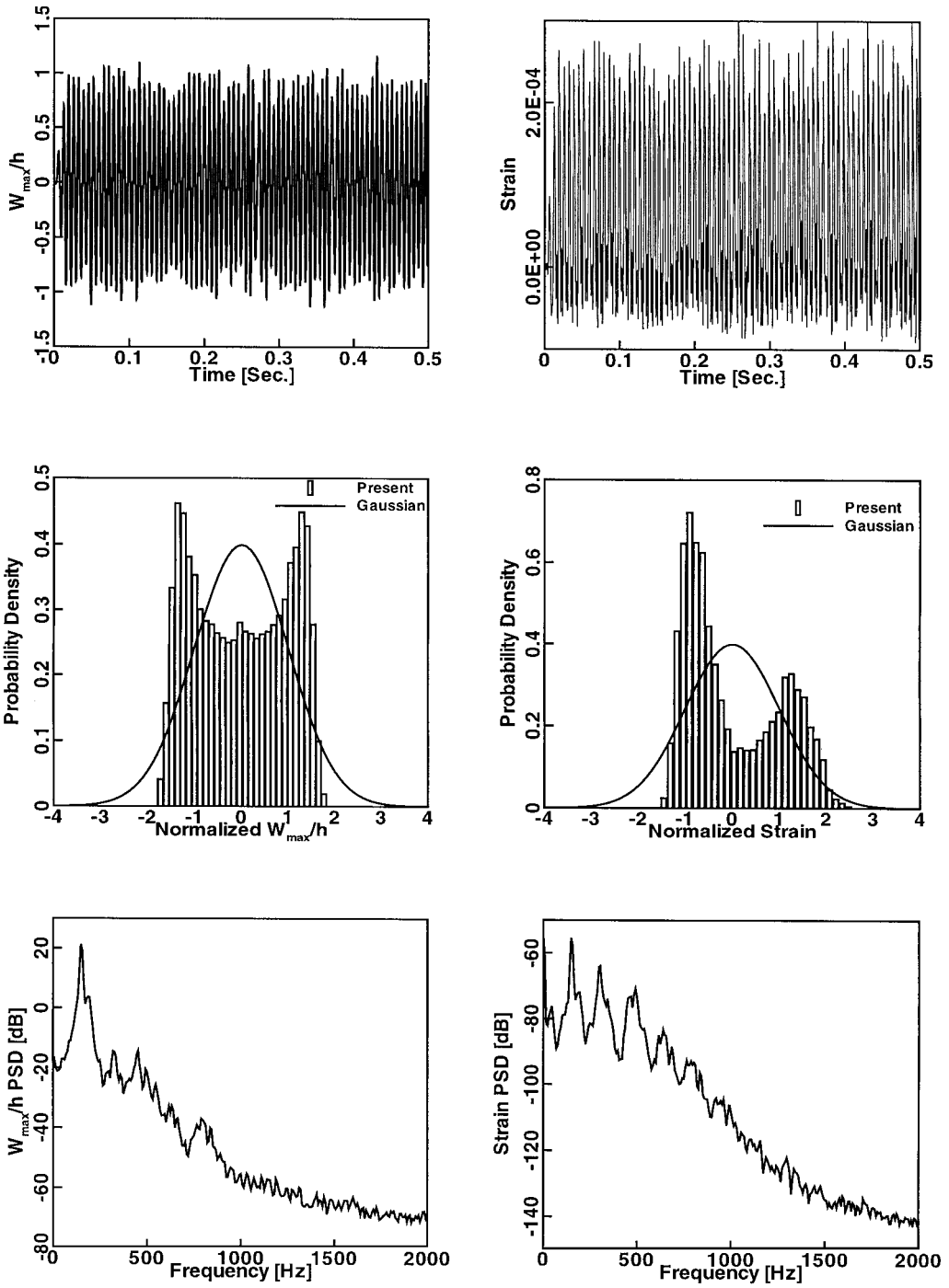

Fig. 7 Random response of a simply supported square isotropic plate at 100 dB SPL and $\lambda = 800$.

SPL = 100 and 120 dB and $\lambda = 0$ (sonic fatigue, points A and B in Fig. 3), respectively. At the low 100-dB SPL, the panel basically experiences a small deflection linear random vibration dominated by the fundamental (1, 1) mode. The panel motion at the high 120-dB SPL, however, is clearly a large deflection nonlinear random vibration. This is demonstrated by the peaks in PSD plots that are broadening and shifting to the higher frequency and by the presence of nonzero-mean in-plane strain shown in the strain plots. The large deviation from the Gaussian distribution is shown by the strain probability plot and the large skewness and kurtosis values for strain.

At $\lambda = 800$ and 0 SPL (panel flutter, point C in Fig. 3), the panel response shown in Fig. 6 is a large-amplitude limit cycle motion. The displacement probability density and the PSD of $(W_{\max}/h)$ both describe a periodic motion. The maximum strain time history and the PSD show clearly the effect of a large inplane strain component due to large amplitude periodic motions.

The panel responses at the combined loads of $\lambda = 800$ and SPL = 100 and 120 dB (points D and E in Fig. 3) are shown in Figs. 7 and 8, respectively. The maximum deflection and strain time histories show the nonlinear large deflection vibrations dominated by the fundamental mode and the presence of inplane strain components.

C. Rectangular Composite Plate

Nonlinear response of composite panels under aerodynamic and acoustic pressures can be determined using the present formulation and solution procedure. As an example, a clamped rectangular graphite–epoxy plate of eight layers $[0/45/-45/90]_s$ is analyzed. The dimensions and material properties of the panel are $a = 15$ in. (38.1 cm), $b = 12$ in. (30.5 cm), $h = 0.048$ in. (0.122 cm), $\rho = 0.1458 \times 10^{-3}$ lb-s^2/in.^{4} (1550 kg/m^3), $\nu_{12} = 0.22$, $E_1 = 22.5$ Msi (155 GPa), $E_2 = 1.17$ Msi (8.07 GPa), $G_{12} = 0.66$ Msi (4.55 GPa), and $G_{23} = 0.44$ Msi (3.03 GPa). The in-plane edges

Table 2 Moments of the W_{max}/h for the simply supported square isotropic plate

SPL, dB	λ	Mean, in./in.	Variance, $in.^2/in.^2$	Skewness, $in.^3/in.^3$	Kurtosis, $in.^4/in.^4$
100	0	0.002832	0.1186	−0.02211	−0.8503
120	0	0.01750	2.5941	−0.03002	−0.2392
0	800	-2.348×10^{-4}	0.4020	-4.756×10^{-4}	−1.450
100	800	7.245×10^{-4}	0.4020	4.915×10^{-4}	−1.371
120	800	-1.257×10^{-3}	0.9123	0.02312	−0.8120

Table 3 Moments of the maximum strain for the simply supported square isotropic plate

SPL, dB	λ	Mean, μin./in.	Variance, $\mu in.^2/in.^2$	Skewness, $in.^3/in.^3$	Kurtosis, $in.^4/in.^4$
100	0	0.6917	428.2	0.07492	−0.7265
120	0	116.5	2.173×10^4	1.650	2.983
0	800	65.73	1.138×10^4	0.4325	−1.413
100	800	62.91	1.132×10^4	0.5225	−1.155
120	800	136.0	1.872×10^4	1.103	0.8306

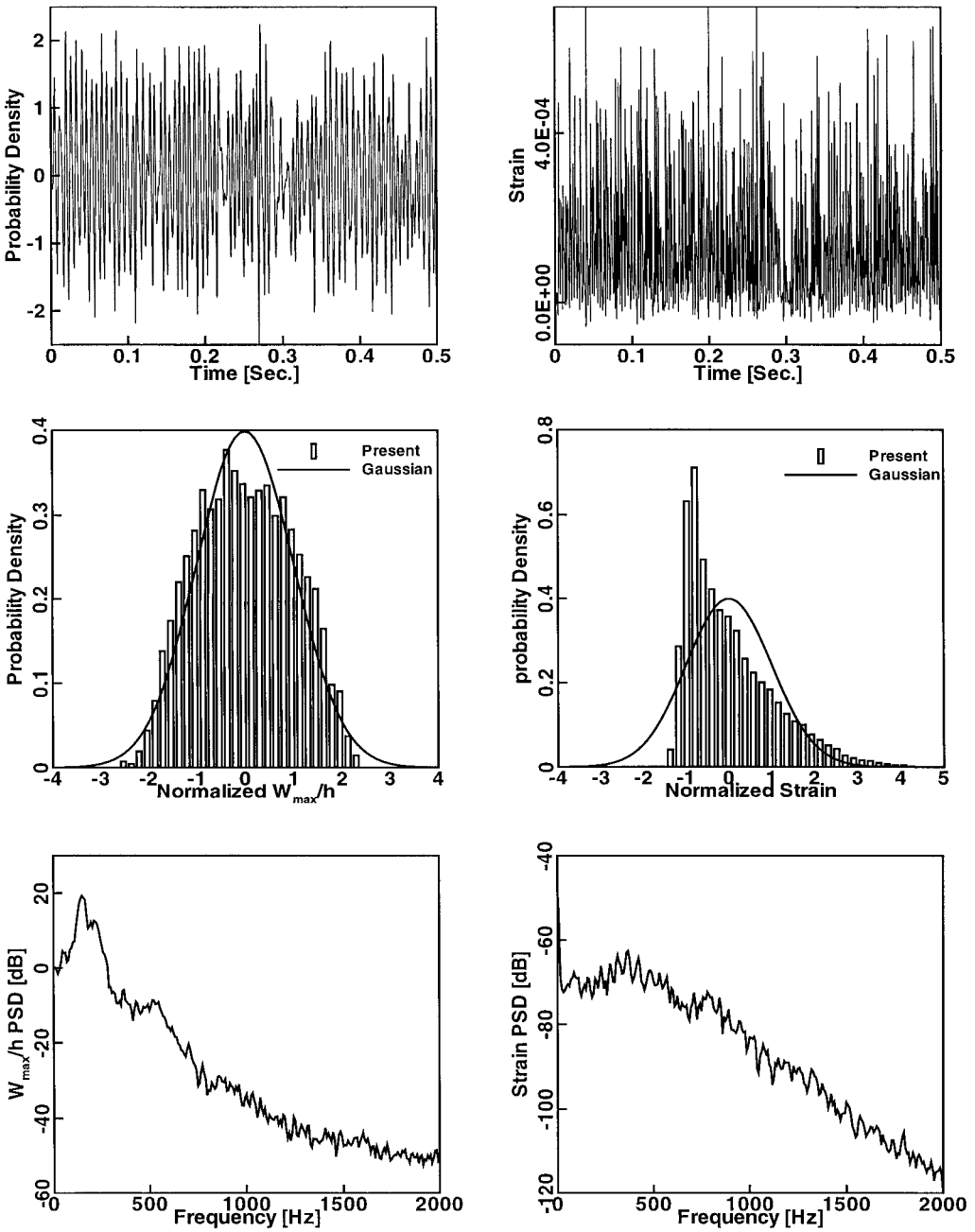

Fig. 8 Random response of a simply supported square isotropic plate at 120 dB SPL and $\lambda = 800$.

are immovable and the plate is modeled with a 12×12 mesh. The number of system equations in structure node DOF $\{W_b\}$ is 363. The system equations are first reduced to the modal coordinates using the lowest n modes in increasing frequency order. The rms W_{max}/h at 120-dB SPL and $\lambda = 800$ using different numbers of modes are shown in Table 4. The results show that a 20- or 25-mode model would yield a converged rms maximum deflection.

To demonstrate the advantage of using the modal participation defined in Eq. (9), the participation values for the 25-mode model are shown in Table 5. By retaining those 13 modes with participation value >1% in the analysis, the rms W_{max}/h is 0.8124 at 120-dB SPL and $\lambda = 800$. Using the 13 most contributing modes, the rms (W_{max}/h) vs nondimensional dynamic pressure λ at SPL of 0, 100, 110, and 120 dB are shown in Fig. 9. Similar conclusions from the isotropic panel can be drawn for the composite panel, that is, at low dynamic pressure ($\lambda \ll \lambda_{cr}$) only acoustic loading needs to be considered, and at significant and high dynamic pressures, both aerodynamic and acoustic loads have to be considered for the design

Table 4 With different number of modes, rms (W_{max}/h) for a clamped rectangular graphite–epoxy panel at 120 dB SPL and $\lambda = 800$

Number of modes n	rms (W_{max}/h)
1	0.5557
2	0.5845
6	0.7814
9	0.7798
16	0.8279
20	0.8110
25	0.8183
Selected 13 modes	0.8124

Table 5 Modal participation values for a clamped rectangular graphite–epoxy panel at 120 dB SPL and $\lambda = 800$ with the lowest 25 modes

Mode number	Participation, %	Mode number	Participation, %
1	36.72	13	0.28
2	5.24	14	4.19
3	19.30	15	0.38
4	4.25	16	0.99
5	4.01	17	1.38
6	7.67	18	2.55
7	1.71	19	0.21
8	0.76	20	0.27
9	0.33	21	0.53
10	1.54	22	0.33
11	4.77	23	0.54
12	0.35	24	0.14
		25	1.54

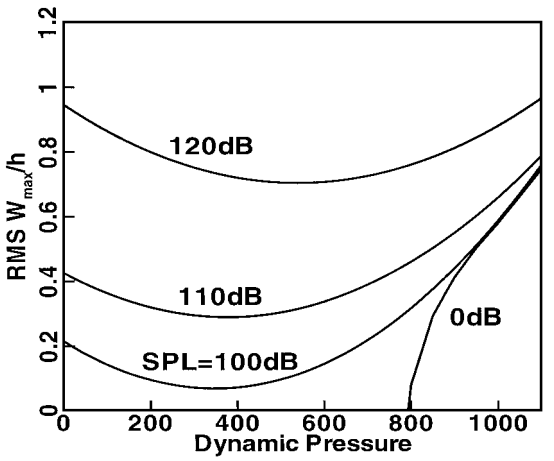

Fig. 9 Clamped rectangular graphite–epoxy plate rms maximum deflection.

and analysis of surface panels at supersonic flow. Response time history, probability distribution, and PSD are not repeated for the composite panel.

IV. Conclusion

A finite element time-domain modal formulation is presented for the analysis of nonlinear response of composite panels subjected to combined acoustic and aerodynamic pressures. The advantage of using modal participation for retaining the most contributing modes was demonstrated. For panels at supersonic flow, only acoustic excitations (sonic fatigue) are to be considered for low ($\lambda \ll \lambda_{cr}$) dynamic pressure, and both acoustic and aerodynamic pressures have to be considered for significant (but $\lambda < \lambda_{cr}$) and high ($\lambda > \lambda_{cr}$) dynamic pressures. Future extension of the present work includes the consideration of combined acoustic, aerodynamic, and thermal loads.

Acknowledgments

The first and second authors would like to acknowledge the partial support by U.S. Air Force Research Laboratory (AFRL) Grant F33615-91-C-3205. The third author would like to acknowledge the support by Grant NAG1-2150 from NASA Langley Research Center and by Contract F33615-98-D-3210 No. 5, AFRL.

References

[1] Vaicaitis, R., "Recent Advances of Time Domain Approach for Nonlinear Response and Sonic Fatigue," *Structural Dynamics: Recent Advances: Proceedings of the 4th International Conference*, edited by M. Petyt, H. F. Wolfe, and C. Mel, Elsevier Applied Science, London, 1991, pp. 84–103.

[2] Vaicaitis, R., "Time Domain Approach for Nonlinear Response and Sonic Fatigue of NASP Thermal Protection Systems," *Proceedings of the AIAA/ASME/ASCE/AHS/ASC 32nd Structures, Structural Dynamics, and Materials Conference*, AIAA, Washington, DC, 1991, pp. 2685–2708.

[3] Clarkson, B. L., "Review of Sonic Fatigue Technology," NASA CR-4587, 1994.

[4] Wolfe, H. F., Shroyer, C. A., Brown, D. L., and Simmons, L. W., "An Experimental Investigation of Nonlinear Behavior of Beams and Plates Excited to High Levels of Dynamic Response," U.S. Air Force Research Lab. WL-TR-96-3057, Wright–Patterson AFB, OH, 1995.

[5] Rudder, F. F., and Plumblee, H. E., "Sonic Fatigue Design Guide for Military Aircraft," Air Force Flight Dynamics Lab., AFFDL-TR-74-112, Wright–Patterson AFB, OH, 1975.

[6] Holehouse, I., "Sonic Fatigue Design Guide Techniques for Advanced Composite Airplane Structures," Air Force Wright Aeronautical Labs., AFWAL-TR-80-3019, Wright–Patterson AFB, OH, 1980.

[7] Arnold, R. R., and Vaicaitis, R., "Nonlinear Response and Fatigue of Surface Panels by the Time Domain Monte Carlo Approach," U.S. Air Force Wright Research and Development Center, WRDC-TR-90-3081, Wright–Patterson AFB, OH, 1992.

[8] Vaicaitis, R., and Kavallieratos, P. A., "Nonlinear Response of Composite Panels to Random Excitation," *Proceedings of the AIAA/ASME/ASCE/AHS/ASC 34th Structures, Structural Dynamics, and Materials Conference*, AIAA, Washington, DC, 1993, pp. 1041–1049.

[9] Dowell, E. H., "Panel Flutter: A Review of the Aeroelastic Stability of Plates and Shells," *AIAA Journal*, Vol. 8, No. 3, 1970, pp. 385–399.

[10] Bismarck-Nasr, M. N., "Finite Element Analysis of Aeroelasticity of Plates and Shells," *Applied Mechanics Reviews*, Vol. 45, No. 12, 1992, pp. 461–482.

[11] Bismarck-Nasr, M. N., "Finite Elements in Aeroelasticity of Plates and Shells," *Applied Mechanics Reviews*, Vol. 49, No. 10, Pt. 2, 1996, pp. s17–s24.

[12] Mei, C., Abdel-Motagaly, K., and Chen, R., "Review of Nonlinear Panel Flutter at Supersonic and Hypersonic Speeds," *Applied Mechanics Reviews*, Vol. 52, No. 10, 1999, pp. 321–332.

[13] Laurenson, R. M., and McPherson, J. I., "Design Procedures for Flutter-Free Surface Panels," NASA CR-2801, 1977.

[14] Zhou, R. C., Xue, D. Y., and Mei, C., "Finite Element Time Domain Modal Formulation for Nonlinear Flutter of Composite Panels," *AIAA Journal*, Vol. 32, No. 10, 1994, pp. 2044–2052.

[15] Mei, C., and Chen, R. R., "Finite Element Nonlinear Random Response of Composite Panels of Arbitrary Shape to Acoustic and Thermal Loads Applied Simultaneously," U.S. Air Force Research Lab. WL-TR-97-3085, Wright–Patterson AFB, OH, 1997.

[16] Robinson, J. H., "Finite Element Formulation and Numerical Simulation of the Large Deflection Random Vibration of Laminated Composite Plates," M.S. Thesis, Dept. of Aerospace Engineering, Old Dominion Univ., Norfolk, VA, Aug. 1990.

[17] Green, P. D., and Killey, A., "Time Domain Dynamic Finite Element Modeling in Acoustic Fatigue Design," *Structural Dynamics: Recent Advances: Proceedings of the 6th International Conference*, edited by N. S. Ferguson, H. F. Wolfe, and C. Mel, Inst. of Sound and Vibration Research, Southampton, England, U.K., 1997, pp. 1007–1026.

[18] Tessler, A., and Hughes, T. J. R., "A Three-Node Mindlin Plate Element with Improved Transverse Shear," *Computer Methods in Applied Mechanics and Engineering*, Vol. 50, No. 1, 1985, pp. 71–91.

[19] Bolotin, V. V., *Random Vibration of Elastic Systems*, Martinus–Nijhoff, Dordrecht, The Netherlands, 1984, pp. 290–292, 314–316.

[20] Chiang, C. K., "A Finite Element Large Deflection Multiple-Mode Random Response Analysis of Complex Panel with Initial Stresses Subjected to Acoustic Loading," Ph.D. Dissertation, Dept. of Aerospace Engineering, Old Dominion Univ., Norfolk, VA, May 1983.

[21] Roberts, J. B., and Spanos, P. D., *Random Vibration and Statistical Linearization*, Wiley, New York, 1990, pp. 178–187.

A. M. Baz
Associate Editor